J Mater Sci: Mater Electron (2017) 28:13937–13949
DOI 10.1007/s10854-017-7243-5

Oxidation rates of aluminium nitride thin films: effect of composition of the atmosphere

Ryszard Korbutowicz[1] · Adrian Zakrzewski[2] · Olga Rac-Rumijowska[1] · Andrzej Stafiniak[1] · Andrej Vincze[3]

Received: 16 March 2017 / Accepted: 29 May 2017 / Published online: 2 June 2017
© The Author(s) 2017. This article is an open access publication

Abstract This paper presents an analysis of thermal oxidation kinetics for Aluminium nitride (AlN) epitaxy layers using three methods: dry, wet and mixed. The structures thus obtained were examined by means of scanning electron microscope, energy-dispersive X-ray spectroscopy, spectroscopic ellipsometry and secondary ions mass spectroscopy. On the basis of the investigation results, a model of layer structure after oxidation was proposed, the thickness of the layers was assessed and the refractive indices for particular layers were determined. The modelling results prove that AlN thermal oxidation in dry oxygen follows the logarithmic law, wet oxidation follows the parabolic law, whereas mixed oxidation follows the linear law.

✉ Ryszard Korbutowicz
ryszard.korbutowicz@pwr.edu.pl

Adrian Zakrzewski
adrian.zakrzewski@pwr.edu.pl

Olga Rac-Rumijowska
olga.rac-rumijowska@pwr.edu.pl

Andrzej Stafiniak
andrzej.stafiniak@pwr.edu.pl

Andrej Vincze
andrej.vincze@stuba.sk

[1] Faculty of Microsystem Electronics and Photonics, Wroclaw University of Science and Technology, Wybrzeże Wyspiańskiego 27, 50–370 Wroclaw, Poland

[2] Faculty of Mechanical Engineering, Wroclaw University of Science and Technology, Wybrzeże Wyspiańskiego 27, 50–371 Wroclaw, Poland

[3] International Laser Centre, Ilkovicova 3, 841 04 Bratislava, Slovakia

1 Introduction

The development of complex III-nitride semiconductor technology has opened up new possibilities of using them in such devices as light emitters and detectors, diodes, and microwave transistors [1]. New MOS- and MIS-based devices are used for the production of gases and other chemical compounds detectors [2, 3]. Here surface passivation must be overcome to stabilise the properties of the gas sensitive surface. The recent literature on this subject includes a significant number of descriptions concerning the phenomena during the thermal dry and wet aluminium oxidation. Among the main techniques for the production of passivation layers on the surface of III-nitride semiconductor devices, the vacuum methods, often plasma-supported, are mentioned. However, a far better solution consists in obtaining oxides of surface layers as a result of controllable oxidation. The gallium nitride GaN oxidation has been long described in the literature [4, 5]. The oxidation of the second nitride, i.e. aluminium nitride, has been learned to a lesser extent, though the interesting properties of the aluminium oxide Al_2O_3 (thermal and chemical stability) indicate that this oxide could be used as the passivation shield. Generally, the oxidation of compound semiconductors, i.e. AIIIBV and AIIIN, poses a number of problems due to the difficulties in describing in detail the reactions that take place during such processes. In particular, this concerns the aluminium compounds, since aluminium is an element showing high affinity to oxygen.

The published papers on the thermal oxidation of semiconductor compounds AIIIN describe largely dry oxidation, while the wet oxidation is described comparatively rarely [4, 5]. There also exists a third method of thermal oxidation, namely mixed oxidation that takes place when a mixture of nitrogen, oxygen and water vapour is fed to the

reactor. In this paper we present the results of thermal oxidation of AlN thin layers deposited on Si(111) substrates by means of the three methods mentioned above. We also aim to present the established parameters of the obtained structures, the analysis of oxidation kinetics in dry, wet and mixed oxidations, and the quality of the obtained aluminium oxide.

2 Materials and methods

Aluminium nitride (AlN) was deposited by means of MetalOrganic Vapor Phase Epitaxy MOVPE (AIXTRON CCS reactor) on Si(111) wafers at a high temperature of 1060 °C. Such layers are not optimised in terms of structural, optical or electrical parameters; they are often used as buffer layers in gallium nitride GaN epitaxy on silicon wafers in order to protect Si against gallium etching at a high epitaxy temperature. The thickness of AlN layers deposited on silicon substrate amounted to ca. 200 nm. The substrates with AlN layers were cut into samples of 10×10 mm^2, cleansed (degreased and the natural oxide was removed from the AlN surface), then they were subjected to thermal oxidation on the stand described in detail in [6]. The processes of oxidation were carried out at a constant temperature of 1012 °C in three gas media of various compositions (gas mixtures):

a. nitrogen N_2 as the carrier gas of a greater purity than 6 N and oxygen O_2 of a purity of 5.5 N as the oxidising media (hereinafter referred to as the dry media)—dry oxidation,
b. nitrogen N_2 as the carrier gas of a greater purity than 6 N and nitrogen N_2 flowing from the saturation unit with hot water as the oxidising media (hereinafter referred to as the wet media)—wet oxidation,
c. containing nitrogen as the carrier gas, oxygen, and water vapour as the oxidising media (hereinafter referred to as the mixed media)—mixed oxidation.

The gas flows were balanced, amounting to ca. 2 l/min. The oxidation processed were conducted at various time frames. In previous papers, the authors demonstrated that the mixed oxidation is fast; therefore, it was carried out at: 10, 20, 30, 40 and 50 min time frames. The other oxidation types (dry and wet) were carried out at 10, 30, 50 and 100 min time frames.

For the microscopic observations, the scanning electron microscope (SEM) Hitachi SU6600 was used. The surface topography was made by SEM, since it offers a greater resolution than optical microscopes. The wavelength of the electron beam is far lesser (<1 nm) than the wavelength of electromagnetic radiation within the range of visible light (400–700 nm). Moreover, SEM microscopes allow for observing material that are translucent in visible light. The maximum resolution of this system equals 1.2 nm (according to the manufacturer).

During the SEM imaging the accelerating voltage amounted to 10 kV and at the working distance about 10 mm (the distance at which the beam is focused). The signal was collected when the scanning beam was perpendicular to the surface and when it was titled by 30° from normal.

The chemical composition of layers was determined using Energy-Dispersive X-ray Spectroscopy (EDS). This technique, like SEM, makes use of the interaction between the electron beam and the surface of the sample. However, it is the X-ray energy spectrum that is subjected to an analysis, not the secondary electrons. The X-ray energy results from the energy difference between electron shell typical of the atoms of each element. The X-ray emission is caused by electrons jump between energy shells as a result of the primary electron beam interaction [7].

The analysis of the surface composition by means of EDS was carried out in the chamber of Hitachi SU6600 microscope using Thermo Scientific NORAN System 7 detector at the accelerating voltage of 5 kV and a working distance of about 10 mm. In order to average the results obtained for the surface chemical composition as well as establish possible material heterogeneity, an area of 125×95 μm^2 was examined. Following this EDS analysis, the distribution of particular elements in the layer was determined.

The thickness of the aluminium oxide layers was determined following a modelling of results made by means of Spectroscopic Ellipsometry (SE) using J.A. Woollam's V-VASE ellipsometer for the spectrum from 300 to 1700 nm with a resolution of 10 nm at three incidence angles of 65°, 70° and 75° This method helps establish the optical parameters and the thickness of particular layers in the samples under investigation within a wide spectral range. By means of the ellipsometry measurements it is also possible to determine the sample surface, e.g. its roughness. Among the advantages of this method, a great sensitivity and non-destructive way of investigation are enumerated. The SE analyses allow for establishing the characteristic features of layers one atom thick.

The general idea behind the ellipsometry measurements is based on an analysis of the polarisation of the light beam reflected from the sample under investigation. The light beam with a linear polarisation is directed at a given angle at the sample. As a result of the reflection, the beam changes its polarisation into an elliptical one. This change depends only and exclusively on the angle of incidence, the wavelength, the thickness of particular layers and their optical properties. It is described by the

ellipsometric parameters, i.e. phase difference Δ and amplitude ratio Ψ. The angles of incidence at which the beam and the sample interact should include the values near to Brewster's angle for which this method is most sensitive. The spectral characteristics of Δ and Ψ parameters make the ellipsometry spectra. The most significant and difficult task consists in extracting interesting values of parameters that could define the sample on the basis of the obtained spectra. To this end, a mathematical model reflecting the characteristics of the sample is created using the ellipsometry software. This model is based on Δ and Ψ parameters that were established during the measurements. The degree of adjusting the model value with the measured values is specified by mean squared error (MSE). From the user's point of view, the mathematical model is created as a result of defining particular layers of the sample. The layers are then defined by their thickness and the values of optical parameters. They might be taken from the ellipsometry material database or created be the user by means of i.a. Cauchy's equation or effective medium approximation layer (EMA). In the case of Cauchy's equation, the refractive index is specified using parameters A_n, B_n and C_n typical of this equation. Additionally, the extinction coefficient κ is determined. For the EMA model, the optical parameters for the materials in a given layer are interpolated. In most cases, the layers are defined on the basis of the contents of air in the base material. Depending on the type of interpolation, Bruggeman's, Maxwell–Garnett's or linear definitions are used. The authors of these results have made use of Bruggeman's definition that is most effective with regard to the properties of the investigated samples.

Moreover, another analysis by means of secondary ion mass spectroscopy (SIMS) was carried out. Time of Flight SIMS (Ion-TOF SIMS IV) in dual beam mode was used to perform depth profiling experiments. A liquid metal ion gun Bi^+ at 25 keV was used as analytical ion gun and Cs^+ at 1 keV with 300 µm × 300 µm size area for sputtering and inside of that 90 µm × 90 µm was the analyzed area. During the measurement, the operation of the flood gun was used in order to minimize the charging effect of the surface.

3 Results and discussion

3.1 Chemical analysis of the oxidation processes

The observations made by means of the scanning electron microscope demonstrated that the surface of the not oxidised AlN layer is rough. The layer consists of continuous areas between which well-formed grains of different sizes can be seen (Fig. 1).

The microstructure of aluminium oxide made as a result of the oxidation process depends both on the process time and the composition of the oxidising agents (Fig. 2). After 10 min of oxidation in dry atmosphere, the surface of the aluminium oxide is made up of crystal grains embedded in the polycrystalline layer (Fig. 2a, b). At the same time, the crystal grains are not clearly seen when the process was carried out in wet (Fig. 2c, d) or mixed atmosphere (Fig. 2e, f), but their microstructure is similar to the microstructure of grains formed in dry oxidation.

The microstructure of aluminium oxide has visibly changed after a long period of oxidation of 100 min in dry and wet atmosphere, and 50 min in nitrogen containing both oxygen and water molecules. The surface of aluminium oxide in dry atmosphere consists of grains that make a network (Fig. 3a). In wet nitrogen and in gas containing nitrogen, oxygen and water vapour, aluminium oxide appears and starts crystallising (Fig. 3b, c).

3.2 Energy-dispersive X-ray spectroscopy

The EDS analyses were carried out for all samples at a relatively small electron beam excitation energy of 5 kV. It was

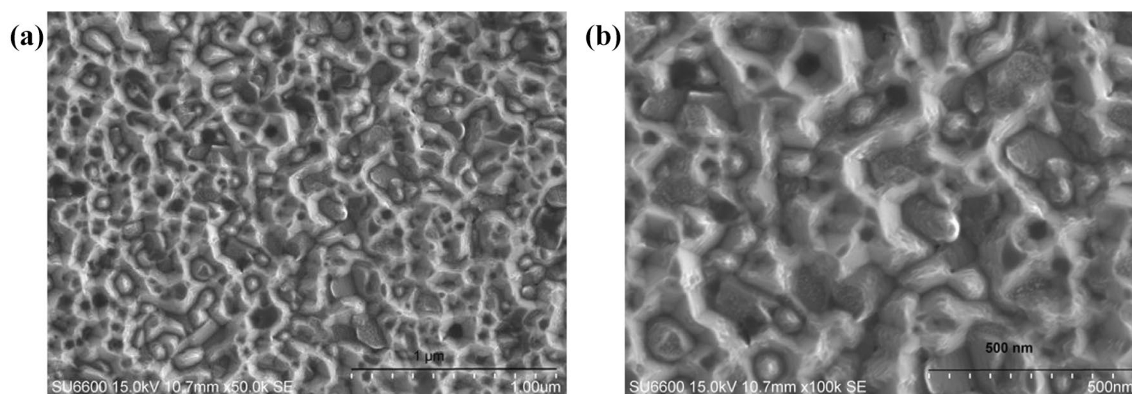

Fig. 1 SEM images of not oxidised AlN layer: **a** 50k, **b** 100k magnification

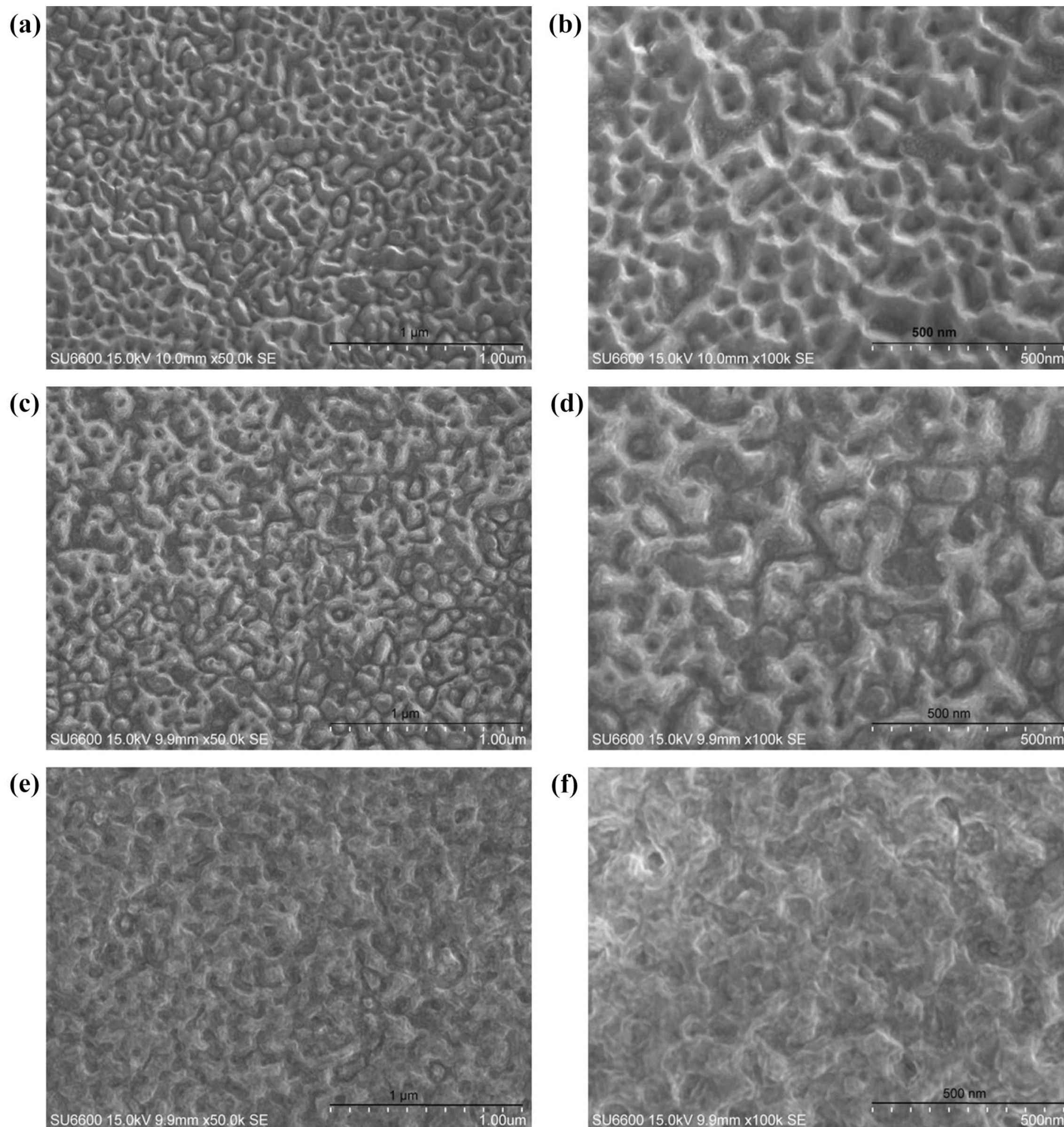

Fig. 2 Microstructure of AlN surface after 10 min of oxidation in various methods: **a** dry 50k; **b** dry 100k, **c** wet 50k, **d** wet 100k, **e** mixed 50k and, **f** mixed 100k magnification

to limit the electron penetration into the sample so that the signal under investigation originated largely from the oxidised layer. However, the excitation energy E_0 must always be slightly greater than the energy of a given X-ray emission line E_c, so called critical ionization energy, in order to conduct effective ionisation and make reliable measurements. In practice, an overvoltage ($E_0/E_c > 1.5$) [7] should be applied, i.e. the value of the excitation beam energy is at least 1.5 times greater than the value of the emission line energy.

Elemental atomic contents in layers were determine for: aluminium, nitrogen, oxygen. We have observed also a weak signal coming from silicon and, sometimes, from carbon. In Fig. 4 are shown an evaluation of elements profiles in samples made by various method of oxidation (all for 50 min of oxidation). The carbon's signal are not shown. The signals measured from not oxidised AlN layer are given for a comparison. Very clearly one can see the increasing of oxygen presence and the vanishing of nitrogen as a relation of oxidation method.

3.3 Spectroscopic ellipsometry

At the first stage of the research, the ellipsometry measurements were carried out on the basis of two samples X and test_AlN as a reference structure. The samples consisted

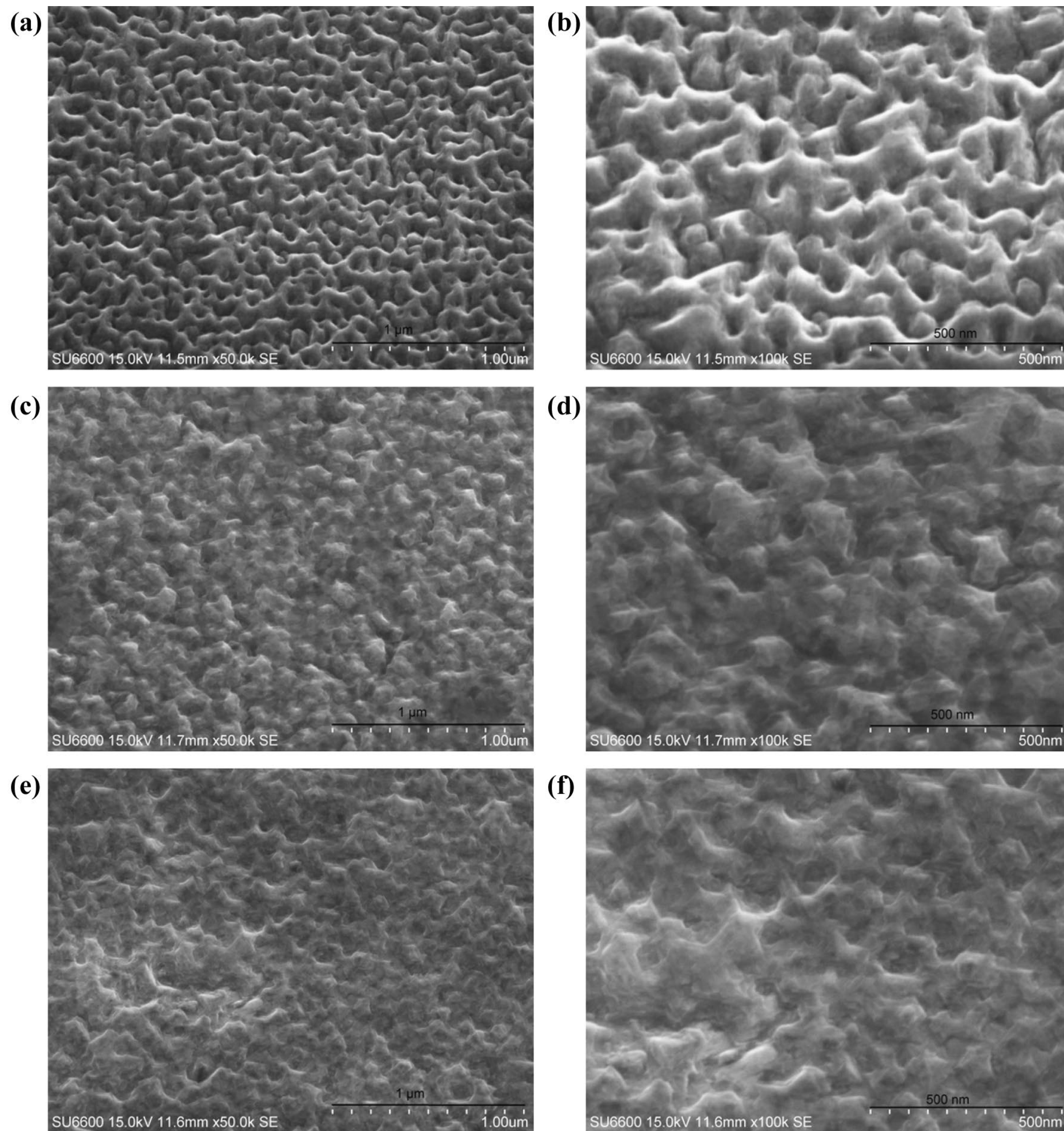

Fig. 3 Microstructure of AlN surface after oxidation in various atmospheres: **a** dry for 100 min 50k; **b** dry for 100 min 100k; **c** wet for 100 min 50k, **d** wet for 100 min 100k, **e** mixed for 50 min 50k and **f** mixed for 50 min 100k magnification

of fragments of substrate with epitaxy structures used for oxidation by means of the mixed method: in mixed media (X) and the dry and wet methods (test_AlN) in dry and wet media respectively. Them after the oxidation process, the other samples were described.

The mathematical models were matched with the results of the ellipsometry measurements for the samples oxidised by means of three methods within different time frames in order to determine the thickness and the optical parameters values, in particular the refractive index of particular layers. On the basis of microscopic examinations of initial modelling results, a four-part structure model was proposed; this model consists of a silicon substrate, aluminium nitride layer infected with oxygen, aluminium oxide layer and a thin surface layer of significant roughness (Fig. 5). The AlN layer to which oxygen diffused was called a layer infected with oxygen. The presence of this element in AlN layer was established using SIMS.

For the purposes of describing AlN layer by means of mathematical modelling, Cauchy's equation was used and the refraction index and extinction coefficient were matched. The Al_2O_3 layer was represented by EMA model that includes the interpolation of variable air content and Al_2O_3 optical coefficient values taken from the

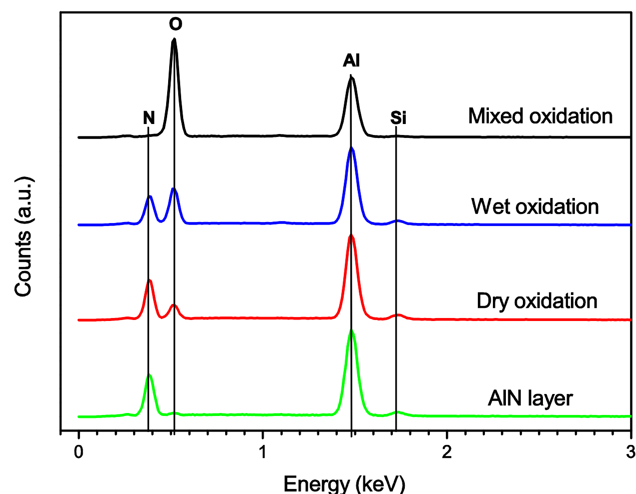

Fig. 4 Diagram of elements profiles evaluation; oxidation time 50 min

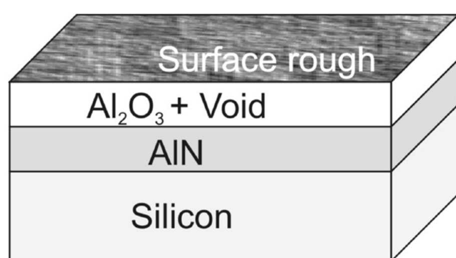

Fig. 5 The scheme of the structures taken for modelling on the basis of the results obtained by means of spectroscopic ellipsometry (SE)

ellipsometry database. The variable air content is a standard method of matching the refraction indices for a layer under investigation. According to the principle in ellipsometry modelling, the rough surface contained 50% of air and 50% of the layer lying directly under it. The AlN Cauchy and Al_2O_3 layers were analysed as gradient layers in terms of optical indices. The gradient ranged from ±5% of the base refractive index and extinction index. The mathematical model thus obtained became the base model for subsequent investigations; the fit of test_aln sample to ellipsometry measurements is presented in Fig. 5. The green curves (dashed lines) present the measurements for three angles, and the red curve (solid line) presents the mathematical model fit. The characteristics include amplitude ratio Ψ (Fig. 6a) and phase difference Δ (Fig. 6b). The MSE value amounted to approx. 12 for the test_ALN sample and 14 for the X sample.

The thickness of particular layers, oxidation time and percentage of air in Al_2O_3 layer is shown in Tables 1, 2 and 3. The acronyms Dt, Wt and Mt means samples subjected to dry (D), wet (W) and mixed (M) oxidation; t means the oxidation time given in minutes.

The mathematical model that describes the oxidised samples used the base model indicated that the thickness of AlN Cauchy layer decreases with oxidation time, while the thickness of Al_2O_3 + Void layer increases. Like in the case of base model, the layers were analysed as gradient layers in terms of optical parameters. The scope of changes ranged from ±5% of the base values of the refraction coefficient and extinction index. The increase in the thickness of Al_2O_3 + Void layer is the greatest during the mixed oxidation, and the least during dry oxidation. However, in the dry type, the least values are also obtained for:

- the air content in Al_2O_3 layer,
- roughness,
- the increase rate for the total layer thickness.

The air percentage in the oxide layer decreases, because the structure becomes more air-tight with oxidation time. After the first oxidation stage, i.e. after 10 min, the thickness of rough surface layer does not change in dry media, slightly increases in wet media, and almost doubly increases in mixed media.

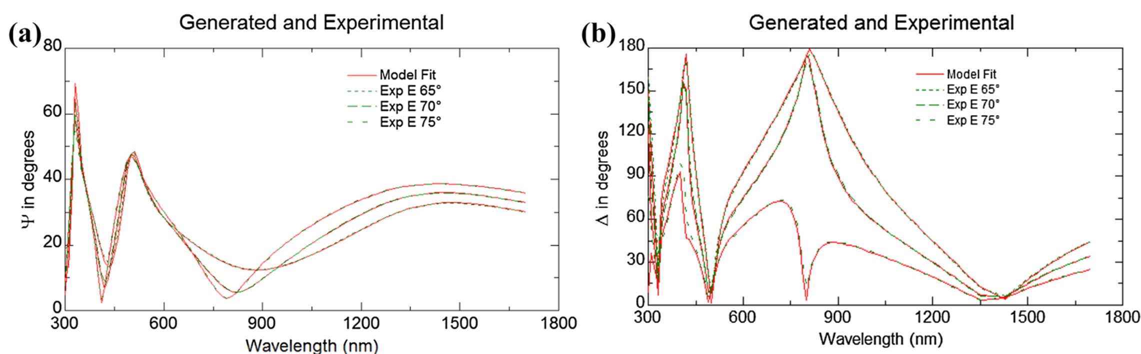

Fig. 6 Mathematical model fit to the results obtained by ellipsometry measurements: **a** amplitude ratio Ψ and **b** phase difference Δ for sample test_AlN (not oxidised AlN/Si)

Table 1 Summary results obtained from SE for the oxidized structures (dry type)

Sample	AlN Cauchy	Al_2O_3 + Void		Surface rough	MSE	All
	Thickness (nm)	Thickness (nm)	Void (%)	Thickness (nm)		Thickness (nm)
test_AlN	208 ± 6	17 ± 5	23 ± 4	5 ± 4	12.52	230 ± 15
D10	178 ± 3	49 ± 6	14 ± 3	5 ± 2	13.80	232 ± 11
D30	175 ± 6	55 ± 10	13 ± 2	5 ± 3	14.88	235 ± 19
D50	171 ± 5	59 ± 9	12 ± 3	6 ± 4	14.90	236 ± 18
D100	163 ± 5	66 ± 4	10 ± 3	6 ± 3	14.75	235 ± 12

Table 2 Summary results obtained from SE for the oxidized structures (wet type)

Sample	AlN Cauchy	Al_2O_3 + Void		Surface rough	MSE	All
	Thickness (nm)	Thickness (nm)	Void (%)	Thickness (nm)		Thickness (nm)
test_AlN	208 ± 6	17 ± 5	23 ± 4	5 ± 4	12.52	230 ± 15
W10	174 ± 3	57 ± 2	17 ± 2	10 ± 2	13.25	241 ± 7
W30	167 ± 2	65 ± 1	15 ± 1	11 ± 1	11.33	243 ± 4
W50	164 ± 2	71 ± 1	13 ± 2	9 ± 1	12.13	244 ± 5
W100	151 ± 2	84 ± 1	11 ± 1	10 ± 1	12.98	245 ± 4

Table 3 Summary results obtained from SE for the oxidized structures (mixed type)

Sample	AlN Cauchy	Al_2O_3 + Void		Surface rough	MSE	All
	Thickness (nm)	Thickness (nm)	Void (%)	Thickness (nm)		Thickness (nm)
X	224 ± 5	22 ± 8	32 ± 9	14 ± 3	14.30	260 ± 16
M10	196 ± 2	53 ± 1	24 ± 1	15 ± 1	4.76	264 ± 4
M20	165 ± 3	89 ± 2	23 ± 1	17 ± 1	8.44	270 ± 6
M30	127 ± 1	131 ± 1	22 ± 0	19 ± 1	4.55	277 ± 3
M40	99 ± 2	165 ± 2	20 ± 1	20 ± 2	9.81	284 ± 6
M50	70 ± 4	197 ± 4	18 ± 0	22 ± 1	4.64	292 ± 9

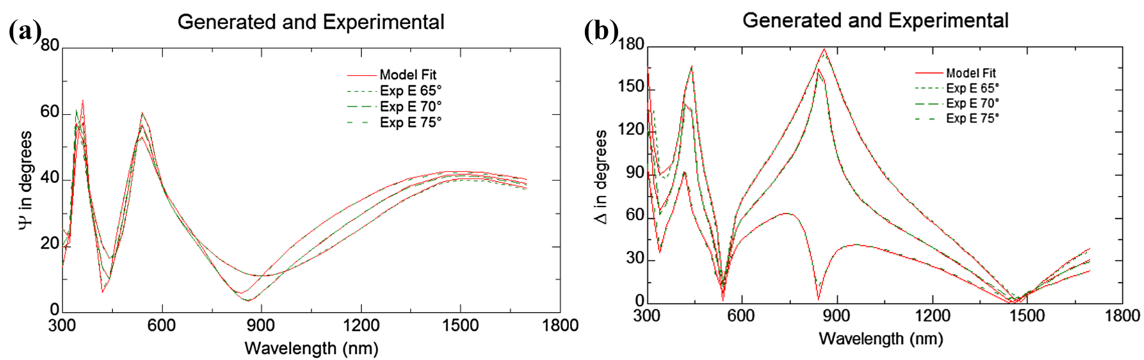

Fig. 7 Mathematical model fits to the results obtained by ellipsometry measurements: **a** amplitude ratio Ψ and **b** phase difference Δ for sample M10

The scheme of changes that take place in particular samples during the oxidation process in different types of media is a result of the analysis of a model fit to ellipsometry measurements; for example, the model fit to ellipsometry measurements for the sample marked by the authors as M10, i.e. subjected to oxidation in mixed media for 10 min (Fig. 7).The values of the refractive index refractive index in layers: AlN Cauchy and Al_2O_3 + Void are presented in Fig. 8. The refractive index of AlN for a sample oxidised by means of the dry method for 50 min, marked as M50, is similar to the table values of the crystallite refractive index Al_2O_3 (Fig. 8a). The refractive index of dry-type

aluminium oxide is the nearest to the crystallite refractive index Al_2O_3 (Fig. 8b). The reason behind it is probably the most tight layer of the oxide of a least roughness.

3.4 Secondary ions mass spectroscopy (SIMS)

Another two samples were examined using Secondary Ions Mass Spectroscopy SIMS. One of the samples was oxidised (D30) in dry media for 30 min (Fig. 9a), the other (W50) in wet media for 50 min (Fig. 9b). The depth of the signal was not determined, since no pattern was known that would allow for determining the depth. However, it is possible to specify the place in the diagram in which AlN changes into a silicon substrate. In the layers under investigation, the presence of oxygen (atoms and particles) was detected at a concentration that changes with the thickness of etched layer (Fig. 9). Although the input thickness of AlN layer was the same, the sputtering time differed owing to a different thickness of Al_2O_3. The thickness of Al_2O_3 layer that appears as a result of oxidation in dry media within 30 min amounts to 55 ± 10 nm (Table 1), whereas in wet media it amounts to 71 ± 1 nm (Table 2). Moreover, aluminium oxide is harder than aluminium nitride, and the sputtering time in order to reach the silicon substrate is longer.

3.5 Mechanism of oxidation AlN

The AlN oxidation reaction is a heterogenic reaction between substrates in the gaseous phase and aluminium nitride in the solid phase. The results of the numerical analysis have demonstrated that at the beginning of the oxidation process (up to 10 min), the aluminium oxide thickness growth rate is not dependent on the oxidation media composition. At this stage, the AlN oxidation process can be best described by a linear oxidation model (Fig. 10c), which means that the oxidation process is controlled by the surface reaction rate.

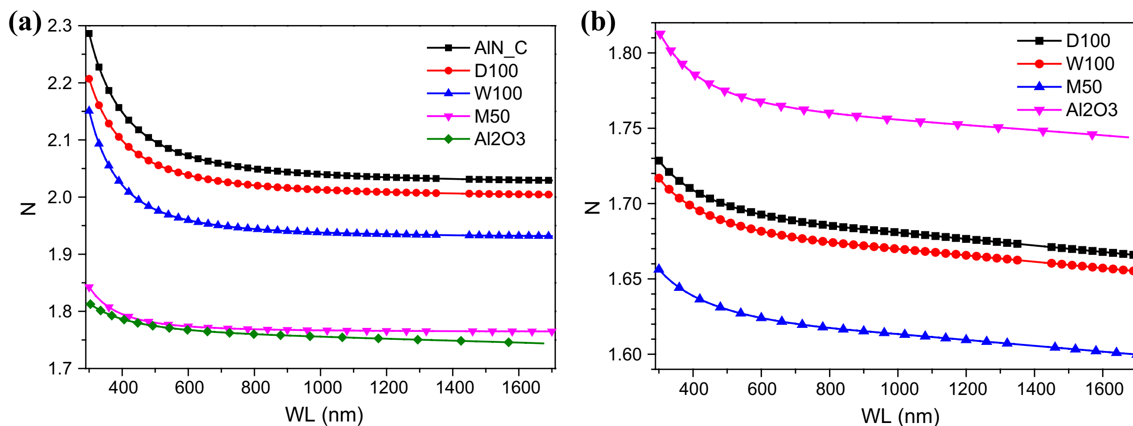

Fig. 8 Spectral characteristics of the refractive indices in layers: **a** AlN Cauchy, **b** Al_2O_3 + Void aluminium oxide

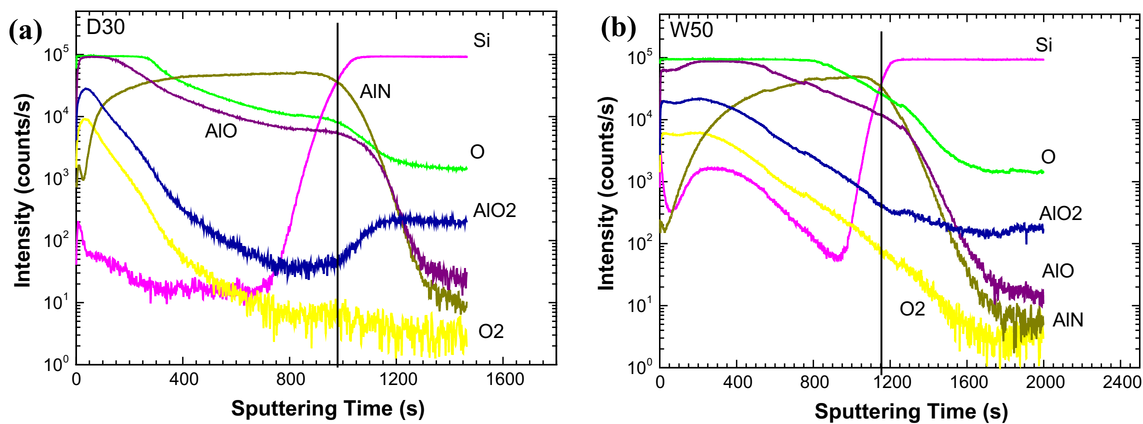

Fig. 9 Profile of element and ion distribution during SIMS sputtering in structures from: **a** dry oxidation for 30 min; **b** wet oxidation for 50 min. A probable AlN/Si boundary was marked with the vertical line

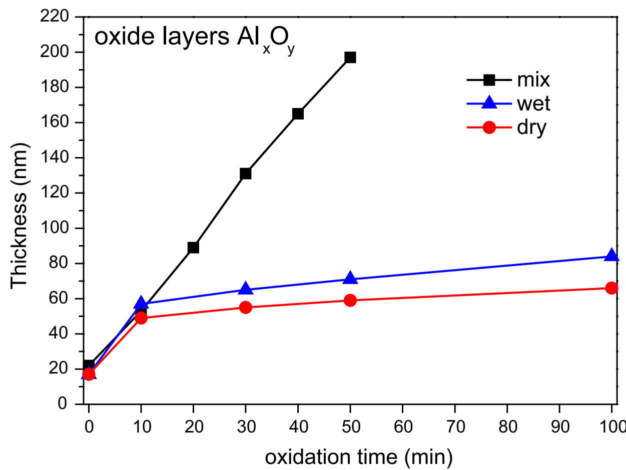

Fig. 10 Change in aluminium oxide thickness during the AlN oxidation process

In the event the oxidation time is longer than 10 min, then the influence of the oxidation atmosphere composition on the AlN oxidation kinetics is more visible (Fig. 11). According to other published research results, at a higher temperature and/or at a longer time, it is the parabolic model that may be used for the description of the oxidation kinetics, since the process is controlled by the reagent transport through the growing aluminium oxide layer [8].

The AlN oxidation process under investigation differs considerably from the metallic aluminium oxidation, owing to the fact that in the former process the gas is released according to reactions Eqs. (1) and (2). In both cases, even at a room temperature, a native oxide layer grows up, since it is a very stable oxide in terms of thermodynamics. In the case of AlN, it was confirmed with a series of analyses by means of the Transmission Electron Microscope, TEM [9], Secondary Ion Mass Spectroscopy, SIMS [10] and Electron Energy Loss Spectroscopy, EELS [11] among others.

During the metallic aluminium oxidation, no additional by-products appear. However, when dry nitrogen with dry oxygen is used, aluminium nitride oxides to Al_2O_3 and nitrogen is produced Eq. (1). This process is commonly described with the following equation:

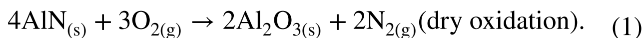

$$4AlN_{(s)} + 3O_{2(g)} \rightarrow 2Al_2O_{3(s)} + 2N_{2(g)} \text{(dry oxidation).} \quad (1)$$

when analysing the gases emitted during the oxidation, Kuromitsu et al. [12] proved that the production of trace amounts of nitric oxides is possible:

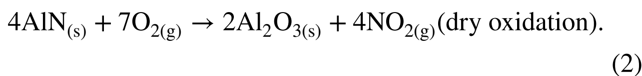

$$4AlN_{(s)} + 7O_{2(g)} \rightarrow 2Al_2O_{3(s)} + 4NO_{2(g)} \text{(dry oxidation).} \quad (2)$$

In the presence of nitrogen and water vapour, AlN oxidises according to the following equation:

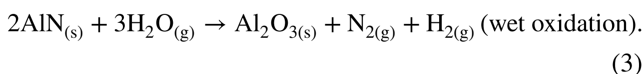

$$2AlN_{(s)} + 3H_2O_{(g)} \rightarrow Al_2O_{3(s)} + N_{2(g)} + H_{2(g)} \text{ (wet oxidation).} \quad (3)$$

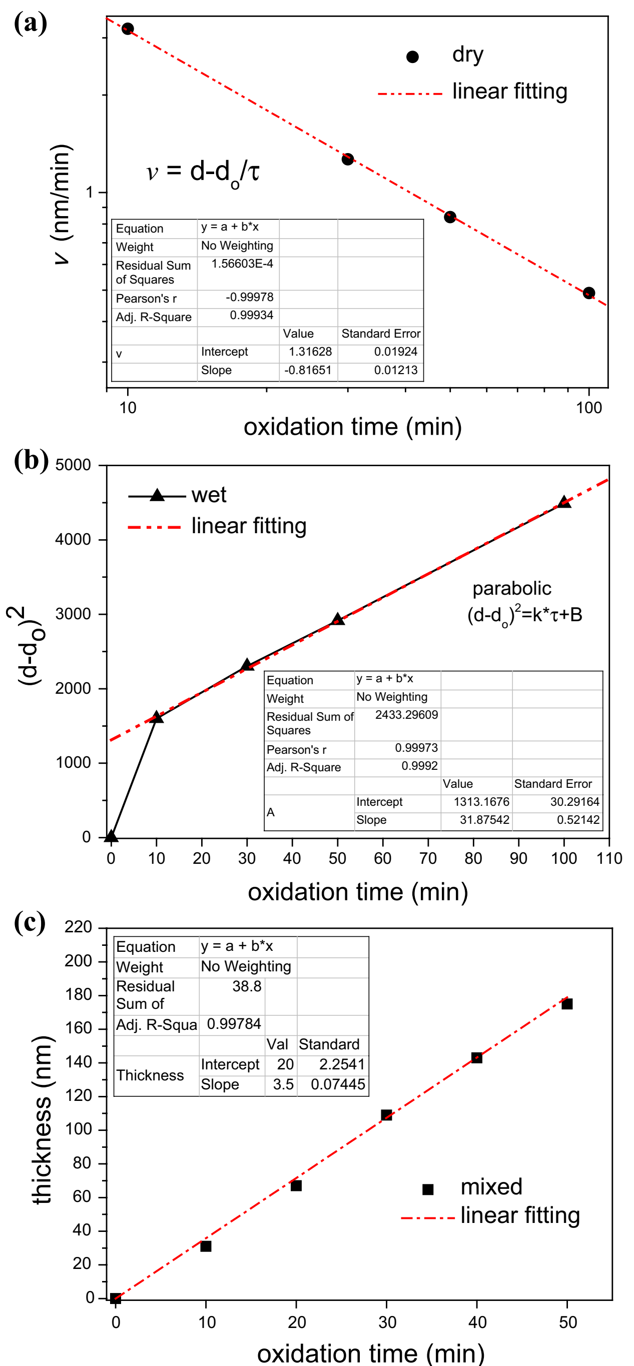

Fig. 11 Change in aluminium oxide thickness during the AlN oxidation process by means of: **a** dry method; **b** wet method; **c** mixed method

In the latter case, hydrogen is a by-product of this reaction Eq. (3). According to thermodynamic equations, $N_{2(g)}$ is more stable than $NH_{3(g)}$ [13]. That is why, it is commonly accepted that it is nitrogen that is produced at a temperature typical of thermal oxidation.

The oxidation of a thin AlN layer takes place because of a series of physical and chemical processes (Fig. 12) which include:

- the oxidant diffusion from the ambient gas to the oxidised surface,
- surface processes: chemisorption, dissociation, surface diffusion with oxidant particles,
- substrate diffusion through the existing oxide layer to oxide/oxidised layer interface, i.e. AlN,
- oxidant/oxidised layer reaction,
- product diffusion through the oxide layer to oxide/gas interface.

In dry and wet atmosphere, the oxidation process follows the logarithmic and parabolic oxidation kinetics (Fig. 11a, b). However, in wet atmosphere the oxidation rate is higher than the oxidation rate in dry one. In mixed atmosphere, the oxidation rate is highest, and this process follows the linear function (Fig. 11). Similar research results are presented in the published literature [12, 14]. According to the data, in wet nitrogen, the AlN oxidation follows the linear function up to 1400 °C.

In this analysis all the oxidation processes were carried out at a constant temperature of 1000 °C and at a constant oxidising agent flow. Therefore, it might be assumed that the gas diffusion rate to the oxide/gas interface is constant and it cannot limit the AlN oxidation process. However, the surface processes including chemisorption, dissociation, and surface diffusion in the presence of oxidant particles/ions have different properties. Dry oxygen is chemisorbed and dissociates to an ionic form of O^{2-} that diffuses through the surface into the volume. If the oxidising gas contains water vapour, then the water dissociation takes place. The surface reaction rate is constant, since the concentration of oxidants does not change with time. Therefore, the analysed processes do not determine the AlN oxidation kinetics.

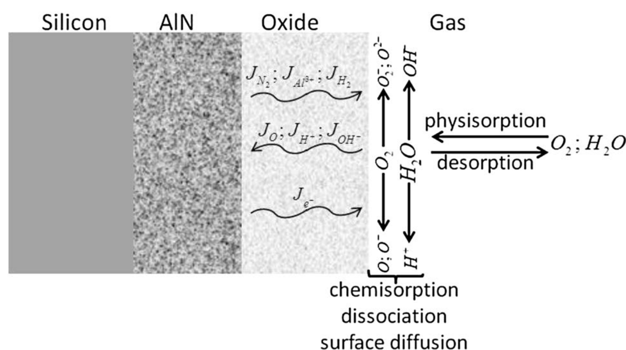

Fig. 12 Scheme of physical and chemical processes during the AlN oxidation

Subsequent processes include substrate and reaction product diffusion through the oxide layer to oxide/oxidised layer and oxide/gas interface (Fig. 13).

Taking into account the microstructure of Al_2O_3 layers, in particular those formed in mixed method (Figs. 2, 3), it may be assumed that AlN oxidation rate is controlled by both substrate and product, and aluminium ions diffusion that takes place at the grain boundaries. Since the aluminium ions diffusion rate through an oxide layer is much less that oxygen diffusion rate [15], it was assumed that oxygen or/and hydroxyl ions diffusion is the controlling process. A greater wet oxidation rate is a result of a greater hydroxyl ions diffusion in comparison to oxygen diffusion. Moreover, Al_2O_3 layer formation in wet nitrogen is more porous, which is related both to the formation of nitrogen, and hydrogen during the reaction Eq. (3).

During the AlN oxidation, oxygen substitutes nitrogen from the crystallite network forming thus interstitial nitrogen. The nitrogen substitution by oxygen is clearly shown in Fig. 14 as a data from EDS analysis.

Therefore, the amount of nitrogen that is released during dry oxidation is not enough to form a sufficient number of pores. Moreover, since the atomic ratio O:Al = 3:2 is greater than N:Al = 1:1, the substitution of 3 oxygen atoms in nitrogen locations generates one vacancy of Al [16]. This may take place as a result of filling the interstitial location with aluminium Eq. (4):

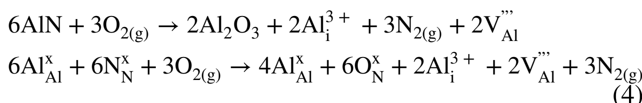

$$6AlN + 3O_{2(g)} \rightarrow 2Al_2O_3 + 2Al_i^{3+} + 3N_{2(g)} + 2V_{Al}^{'''}$$
$$6Al_{Al}^{x} + 6N_{N}^{x} + 3O_{2(g)} \rightarrow 4Al_{Al}^{x} + 6O_{N}^{x} + 2Al_i^{3+} + 2V_{Al}^{'''} + 3N_{2(g)} \quad (4)$$

The density of formed aluminium oxide is greater than the density of aluminium nitride, the molar mass of the oxide is greater as well; therefore, no significant growth in total thickness is seen, except for the oxidised layers in mixed atmosphere (Fig. 15a). Only using this oxidation method, the linear growth of surface roughness is visible along with the growth of the aluminium oxide thickness (Fig. 15b).

In dry method, the surface roughness changes but slightly during the oxidation process. The surface roughness of the aluminium oxide formed in wet gases is about twice as great in comparison to the oxide formed in dry media.

The roughness of the aluminium oxide surface when this oxide forms in wet nitrogen is also seen in SEM images of the sample cross-section after 40 min of oxidation (Fig. 16). Moreover, the images demonstrate a clearly visible polycrystalline, porous microstructure of the forming aluminium oxide.

The formation of the high nanoporosity α-alumina during the oxidation carried out in the presence of water vapour was described by Opila et al. [17]. Water vapour

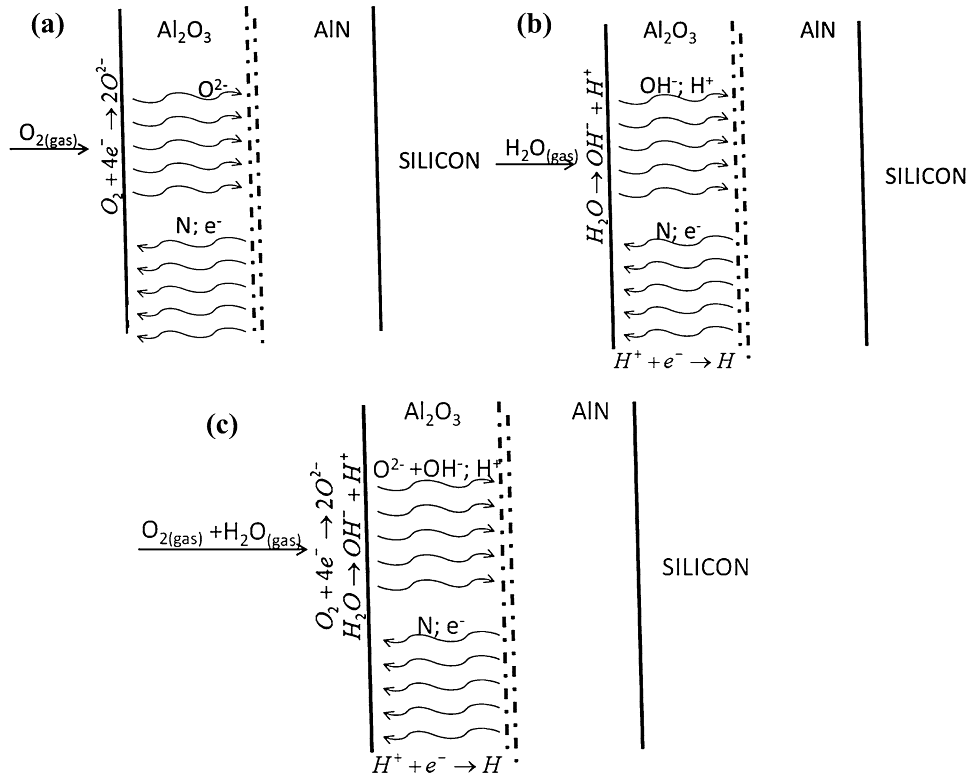

Fig. 13 Scheme of processes during the aluminium nitride oxidation

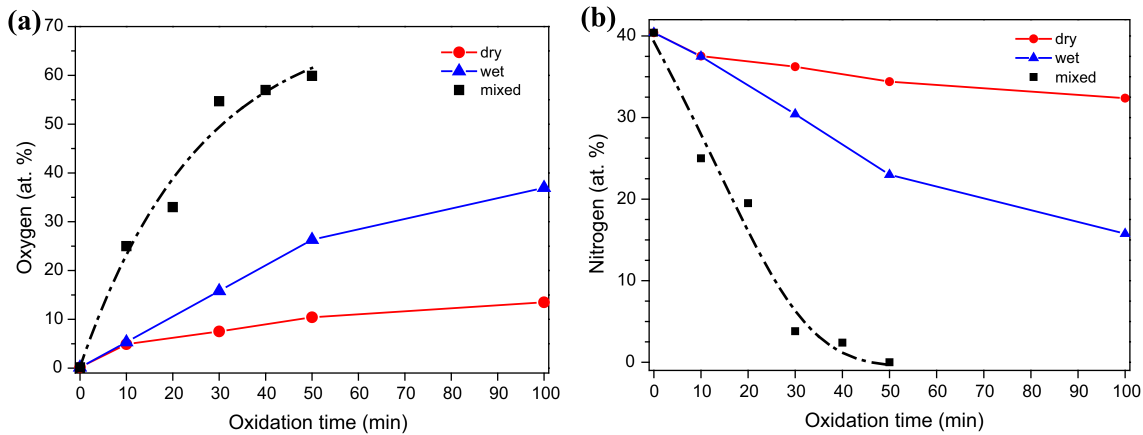

Fig. 14 Change of the content of elements in investigated structures (from EDS analysis): **a** increasing of oxygen amount, **b** decreasing of nitrogen amount

affects the oxidation of oxide-forming material in three ways [18]:

- it increases indirectly the oxidation rate, accelerating the contamination transfer to the forming oxide,
- it increases directly the oxidation rate of materials whose oxides dissolve well in water vapour,
- it reacts with oxides when they grow, forming different hydroxyl compounds.

In the cases under investigation, the AlN layer contained no admixtures; that is why water vapour cannot cause increase directly the oxidation rate. The other ways of affecting AlN oxidation rate by water vapour are related. Water vapour reacts with numerous materials, metal oxides and other metal compounds, forming stable hydroxides like:

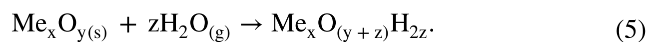

$$Me_xO_{y(s)} + zH_2O_{(g)} \rightarrow Me_xO_{(y+z)}H_{2z}. \quad (5)$$

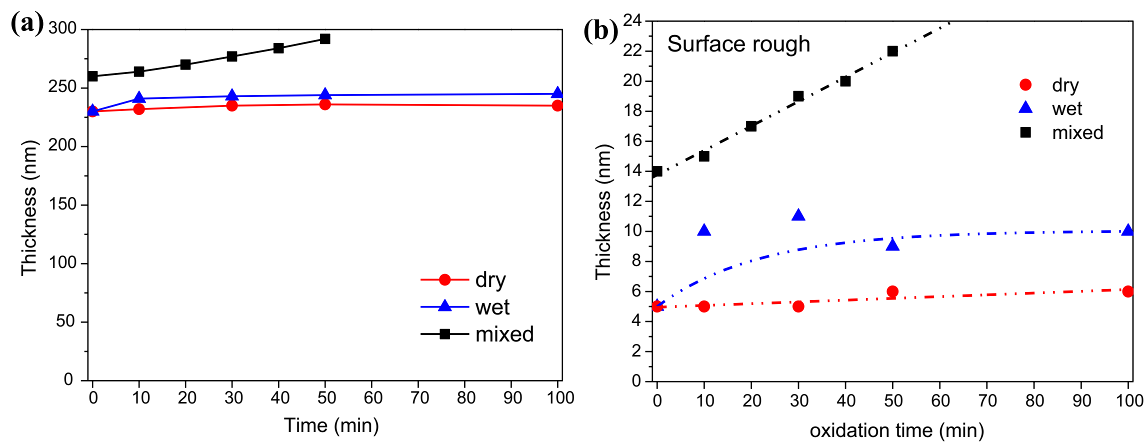

Fig. 15 Change in: **a** total layer thickness; **b** aluminium oxide surface roughness during the AlN oxidation process in dry, wet and mixed media

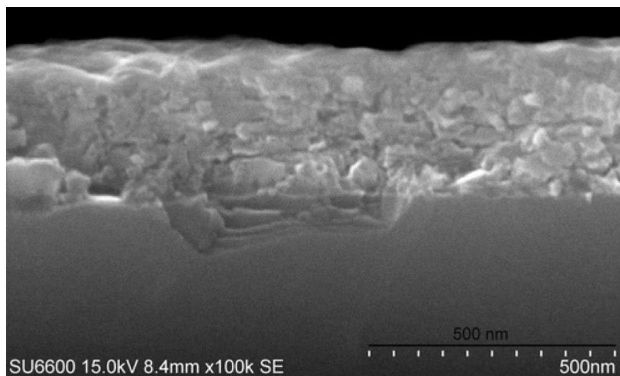

Fig. 16 Cross-section of a sample oxidised for 40 min in wet atmosphere

In the case of aluminium oxide, this property is commonly used in designing humidity sensors [19, 20]. When metal hydroxides decompose, hydrogen appears. By way of analogy to wet silicon oxidation, it may be assumed that hydrogen as a product of reaction Eq. (3) is partly trapped in Al_2O_3. Consequently, the porosity of Al_2O_3 forming in wet media increases along with the diffusion rate of the oxidant to AlN. If AlN oxidation process is carried out in wet nitrogen, it is the lack of effective oxidant like oxygen that determines the oxidation rate. Though the diffusion rate of hydroxyl ions is considerably greater than oxygen, the AlN oxidation rate in wet atmosphere is slightly greater than in dry gases [15]. In mixed method, it is oxygen that is responsible for a fast forming process of aluminium oxide that consequently reacts with hydroxyl ions forming hydroxides. With time they decompose, water separates, and recrystallization takes place. That is why, the aluminium oxide layers forming in the presence of water vapour are more crystal (Fig. 3).

The nature of porous layer of aluminium oxide has also been explained in relevant literature on the basis of visible cracks in the aluminium oxide layer during the oxidation process [12, 14]. However, no cracks were observed during the presented analyses, since the layers were thin and the oxidation time relatively short.

4 Conclusions

This paper presents an analysis of thin epitaxial HT AlN layers subjected to dry, wet and mixed oxidation. The layers were investigated using SEM, EDS, ES and SIMS methods. It was established that thin non-optimised AlN layers are polycrystalline and porous. Such microstructure enables the penetration with oxidising agents. As a result, a quick diffusion occurs and an oxygen gradient in AlN layers is observable: aluminium nitride inside seems infected with oxygen. Then the surface of aluminium oxide layer reveals a high porosity. It reaches highest values after mixed oxidation, and least values after dry oxidation. Similar Al_2O_3 microstructure is needed for humidity and gas sensors. The analysis of dry, wet and mixed oxidation kinetics showed that during the initial 10 min of the process, the process course is similar, notwithstanding the oxidant, the oxide growth rate are for all practical purposes the same. Longer processes reveal that the oxide growth rate in dry oxidation can be described as a logarithmic relationship, while in wet oxidation as a parabolic relationship. However, the oxidation in the presence of oxygen and water vapour (mixed oxidation) is the fastest and is a linear relationship.

Acknowledgements This research was partially supported by Wroclaw University of Science and Technology statutory grant; VEGA 1/0907/13 from the Scientific Grant Agency of the Ministry of Education, Science, Research and Sport of the Slovak Republic.

Compliance with Ethical Standards

Conflict of interest The authors declare that there is no conflict of interest regarding the publication of this article.

Open Access This article is distributed under the terms of the Creative Commons Attribution 4.0 International License (http://creativecommons.org/licenses/by/4.0/), which permits unrestricted use, distribution, and reproduction in any medium, provided you give appropriate credit to the original author(s) and the source, provide a link to the Creative Commons license, and indicate if changes were made.

References

1. S.J. Pearton, J.C. Zolper, R.J. Shul, F. Ren, GaN, Processing, defects, and devices. J. Appl. Phys. **86**, 1–78 (1999)
2. Y. Nakano, T. Jimbo, Interface properties of thermally oxidized n-GaN metal-oxide-semiconductor capacitors. Appl. Phys. Lett. **82**, 218–220 (2003)
3. P. Bidzinski, M. Miczek, B. Adamowicz, Ch. Mizue, T. Hashizume, Impact of interface states and bulk carrier lifetime on photocapacitance of metal/insulator/GaN structure for ultraviolet light detection. Jpn. J. Appl. Phys. **50**, 04DF08 (2011)
4. R. Korbutowicz, J. Prażmowska, in *Semiconductor Technologies* ed. by J. GRYM,Wet thermal oxidation of GaAs and GaN. (In-Tech, Vukovar, 2010). p. 105
5. H.S. Oon, K.Y. Chong, Recent development of gallium oxide thin film on GaN. Mater. Sci. Semicond. Process. **16**, 1217–1231 (2013)
6. R. Korbutowicz, J. Prażmowska, Z. Wągrowski, A. Szyszka, M. Tłaczała, Wet thermal oxidation for GaAs, GaN and Metal/GaN device applications. Proceedings of ASDAM, Smolenice, (2008). pp. 163–166 (2008)
7. J. Goldstein, D.E. Newbury, D.C. Joy, C.E. Lyman, P. Echlin, E. Lifshin, L. Sawyer, J.R. Michael, *Scanning Electron Microscopy and X-Ray Microanalysis*, 3rd edn. Springer, New York
8. LPH Jeurgens, W.G. Sloof, F.D. Tichelaar, E.J. Mittemeijer, Growth kinetics and mechanisms of aluminum-oxide films formed by thermal oxidation of aluminum. J. Appl. Phys. **92**, 1649–1656 (2002)
9. I. Dutta, S. Mitra, L.J. Rabenberg, Oxidation of sintered aluminum nitride at near-ambient temperatures. J. Am. Ceram. Soc. **75**, 3149–3153 (1992)
10. R. Yue, Y. Wang, Y. Wang, C. Chen, SIMS study on the initial oxidation process of AlN ceramic substrate in the air. Appl. Surf. Sci. **18**, 73–78 (1999)
11. M. MacKenzie, A.J. Craven, Quantifying the oxidation of AlN using electron energy loss spectroscopy. J. Phys. D. **33**, 1647–1655 (2000)
12. Y. Kuromitsu, H. Yoshida, S. Ohno, H. Masuda, H. Takebe, K. Morinaga, Oxidation of sintered aluminium nitride by oxygen and water vapor., J. Ceram. Soc. Jpn. **100**, P0–P74 (1992)
13. T. Sato, K. Haryu, T. Endo, M. Shimada, High-temperature oxidation of silicon nitride-based ceramics by water vapour. J. Mater. Sci. **22**, 2277–2280 (1987)
14. H.E. Kim, A.J. Moorhead, Oxidation behavior and flexural strength of aluminum nitride exposed to air at elevated temperatures. J. Am. Ceram. Soc. **77**, 1037–1044 (1994)
15. U. Brossmann, R. Würschum, U. Södervall, H.E. Schaefer, Oxygen diffusion in ultrafine grained monoclinic ZrO_2. J. Appl. Phys. **85**, 7646–7656 (1999)
16. J.H. Harris, R.A. Youngman, R.G. Teller, On the nature of the oxygen-related defect in aluminum nitride. J. Mater. Res. **5**, 1763–1773 (1990)
17. E. Opila, N. Jacobson, D. Humphrey, T. Yoshio, K. Oda, *High Temperature Corrosion and Materials Chemistry* eds. by P.Y. Hou, M. Mc Nallan, R. Oltra, E.J. Opila, D.A. Shores, (The Electrochemical Society, Inc., Pennington, 1998), pp. 430–437
18. R. Riedel, I.W. Chen, *Ceramics Science and Technology*, vol. 4. Applications. (Wiley, Weinheim, 2013)
19. Z. Chen, C. Lu, Humidity sensors, a review of materials and mechanisms. Sens. Lett. **3**, 274–295 (2005)
20. B. Cheng, B. Tian, C. Xie, Y. Xiao, S. Lei, Highly sensitive humidity sensor based on amorphous Al_2O_3 nanotubes. J. Mater. Chem. **21**, 1907–1912 (2011)